# PAPER 3

Geothermics 65 (2017) 60–71

Contents lists available at ScienceDirect

Geothermics

journal homepage: www.elsevier.com/locate/geothermics

# Thermal conductivity map of the Avila region (Spain) based on thermal conductivity measurements of different rock and soil samples

Cristina Sáez Blázquez*, Arturo Farfán Martín, Ignacio Martín Nieto, Pedro Carrasco García, Luis Santiago Sánchez Pérez, Diego González Aguilera

*Department of Cartographic and Land Engineering, University of Salamanca, Higher Polytechnic School of Avila, Hornos Caleros 50, 05003 Avila, Spain*

ARTICLE INFO

*Article history:*
Received 18 May 2016
Received in revised form 3 August 2016
Accepted 2 September 2016

*Keywords:*
Thermal conductivity
Map
Geothermal heat pumps
Low-cost method

ABSTRACT

A thermal conductivity map constitutes an important basis with regards to the design and performance of geothermal heat pump installations. Although the execution of a Thermal Response Test means an ideal solution as it provides the average value of the thermal conductivity over the length of the borehole drilled for the BHE, in small projects it is not possible to carry out these tests because they involve a huge increase of the total budget of the user. This study describes a systematic methodology to produce a thermal conductivity map of an area geographically placed in the center of Spain, the province of Ávila. As a result, a map of thermal conductivity distribution of local rocks is proposed.



## 1. Introduction

The use of geothermal energy is at a point of rapid growth and is expected to continue growing in the future. With respect to Spain, this energy is basically used to generate sanitary hot water (SHW) and/or heat/cool a certain space. The geothermal electric generation in this country is at a very early stage although at the moment, it is being developed in areas like Tenerife where, because of its thermal characteristics, the first Spanish geothermal electric central is going to be placed.

At user level, the very low temperature geothermal energy is used in the production of SHW or heating. For both uses, a careful design of the geothermal installation is required; one of the essential parameters that is decisive is the thermal conductivity of the ground where the installation will be placed. When measuring this parameter, a "Thermal Response Test" (TRT) is needed in order to get accurate values of the whole subsoil to the right design of the geothermal installation. However, in spite of providing this value directly, this test involves an important rise of the price of implementation of a geothermal installation, of little significance (from an economical point of view) at big projects but unviable at small installations. In case of not making this essay, the most usual is not to determine the thermal conductivity of the land and consider the most unfavorable case, that is to say, that value of thermal conductivity (for the type of soil-rock where the installation is located) that requires the highest heat pump power (in function of theoretical tables), rising equally the global budget (Blázquez et al., 2016; Peláez et al., 2014).

In the present paper, measurements of the thermal conductivity of different samples of the characteristic geological materials that occur in the province of Ávila were carried out in the laboratory. Data obtained in soils were compared with the ones obtained by the use of the program ThermoMap developed by a diverse combination of institutions (*GeoZentrum, BRGM, ISOR, MFGI, IGR, BGS, EGEC, RBINS-GBS, REHAU, GBI, PLUS, IGME*) (Thermo Map, 2013). Data acquired in the laboratory and in the case of soils also verified by ThermoMap have allowed generating thus, a thermal conductivity map of the mentioned province. This knowledge will make possible to improve the design of the geothermal heat pump installations (Vijdea et al., 2014; Galgaroa et al., 2015; Clauser and Huenges, 1995; Barry-Macaulay et al., 2013).

The purpose of this study is to obtain values of thermal conductivity by measurements in the laboratory and using the program ThermoMap (only in the case of soils), representative of the Ávila region, to be presented as a thermal conductivity detailed map. For that, a procedure of localization, collection and preparation of samples at the laboratory and analysis of the thermal conductivity parameter of each one of the samples was developed. Thermal conductivities of soils were also estimated by the calculator ThermoMap to carry out a comparison of both methods in these samples.

* Corresponding author.
*E-mail address:* u107596@usal.es (C. Sáez Blázquez).

http://dx.doi.org/10.1016/j.geothermics.2016.09.001

This map of thermal conductivities can be used along with the corresponding geological data, as basic information at the design phase of a geothermal heat pump project (Jackson and Taylor, 1986).

## 2. Materials and methods

### 2.1. Study site

As it has already been mentioned, the determination of the thermal conductivity parameter has been carried out on the most representative geological materials that are part of the province of Ávila; therefore, the map obtained as a result of this study will reflect an analysis of the geothermal situation of the province (in terms of thermal conductivities of the materials) and the possibilities of making use of this energy in this place (Fig. 1).

The Geological and Mining Institute of Spain "IGME" puts at the disposal of the users geological information of all the regions of Spain, in this way, this country is divided into a series of grids to scale 1:50.000 that contain the geology of the area represented. By graphic design software the grids that divide the province of Ávila were digitized and overlapped with the aim of locating each one of the materials found in the study area and calculating the expanse taking up by each one of them. Fig. 2 shows the rock types of this province (Geological and Mining Institute of Spain (IGME), 1972–2003).

As shown in Fig. 2, the province of Ávila is geologically formed by two clearly defined blocks:

- On the one hand, materials belonging to the Hercynian Massif, constituted by igneous rocks from the Upper Carboniferous-Low Permian (mainly granitic rocks) and metamorphic rocks from the Pre-Cambrian-Low Cambrian.
- On the other hand, there is a block constituted by sedimentary materials from the Mesozoic, Tertiary and Quaternary, located in the oriental area of the Amble's valley (Ávila) (César et al., 2014).

Additionally, Table 1 contains the list of materials that constitute the province represented in Fig. 2, the area taken up by each one of them expressed in: area unities ($m^2$) and as percentage (%) with respect to the total area of the province. It can be observed in this Table 1 that, more than half of materials placed in this province have granitic origin.

### 2.2. Sample collection

Due to the lack of information about the thermal conductivity properties of the materials of Ávila, a sampling selecting different sample collection points according to the rock type, lithology and geographical position was carried out. In this way, representative samples of the formations of this region were taken. Given the difficulty to measure the thermal conductivity property "in situ", samples were moved to the lab where, after opportune preparation, measurements were made. Basically two types of rocks have been collected and investigated: solid (rock) and unconsolidated (soil). With the aim of reproducing the conditions of the materials in nature, measurements of thermal conductivity were carried out for different states of water content, in those materials that allow changing its humidity (i.e. soils).

Fig. 3 shows the points where the samples representative of each material presented in Table 1 were taken. As it can be observed, for the same rock type, four different samples were collected with the object of getting a more precise determination of the mentioned thermal conductivity property and the correspondent geothermal map of the province. For three of the investigated rock types (leucogneiss, gneiss and quartzite) the four samples collected for these rocks come from sites next to each other due to the short area taken up by these materials.

### 2.3. Thermal conductivity measurements

#### 2.3.1. KD2 Pro equipment

Equipment used at the measuring of thermal conductivities was the thermal properties analyzer commercially known as KD2 Pro developed by Decagon Devices (Decagon Devices, 2016). It is constituted by a portable controller and a certain sensor (RK-1) usually used in geothermal practice and customarily termed "*needle probe*" that make possible the measuring of two thermal properties: the thermal resistivity and the focus parameter of this work; the thermal conductivity. Its operation is based on the infinite line heat source theory and calculates the thermal conductivity by monitoring the dissipation of heat from the needle probe. Heat is applied to the needle for a set heating time, $t_h$ and temperature is measured in the monitoring needle during heating and for an additional time equal to $t_h$ after heating. The temperature during heating is computed from Equation (1).

$$T = m_0 + m_2 t + m_3 lnt \tag{1}$$

Where:

$m_0$ is the ambient temperature during heating

$m_2$ is the rate of background temperature drift

$m_3$ is the slope of a line relating temperature rise to logarithm of temperature

Equation (2) represents the model during cooling.

$$T = m_1 + m_2 t + m_3 ln\frac{t}{t - t_h} \tag{2}$$

The thermal conductivity is computed from Equation (3).

$$k = \frac{q}{4m_3} \tag{3}$$

$q$ is the heat flux applied to the needle probe for a set time. This heat dissipates along the sample in a different way so and as it can be seen in Equation (3), this value is used by the equipment KD2 Pro to calculate the thermal conductivity value of the sample in question. However, KD2 Pro does not provide the heat flux applied and it only supplies the final thermal conductivity value.

Since these equations are long-time approximations to the exponential integral equations, only the final 2/3 of the data collected are used (ignoring early-time data) during heating and cooling. This approach has several advantages; the effects of contact resistance appear mainly in these early time data, so by analyzing only the later time data the measurement represents better the thermal conductivity of the sample. Also, Equations (1) and (2) can be solved by linear least squares, giving a solid and more adjusted result (Kluitenberg et al., 1993; Shiozawa and Campbell, 1990).

In this study, the RK-1 probe (3.9 mm in diameter and 6 cm in length) has been used to measure the thermal conductivity of the different materials placed in the province of Ávila. This probe is capable of measuring the thermal conductivity between the range of 0.1 and 6 W/mK and ±10% of accuracy.

Additionally, KD2 Pro calculates the accuracy of each measurement by comparing the experimental temperature data to the modelled temperature predicted by the analytical solution of infinite line source theory (Carslaw and Jaeger, 1959). The difference between experimental and modelled temperature is displayed as the coefficient of correlation. It must be clarified that this error term is not a statistical indicator of the measuring quality, but it serves as a qualitative indicator.

The long read times for the RK-1 sensor help to prevent errors caused by effects from the large diameter needle and contact

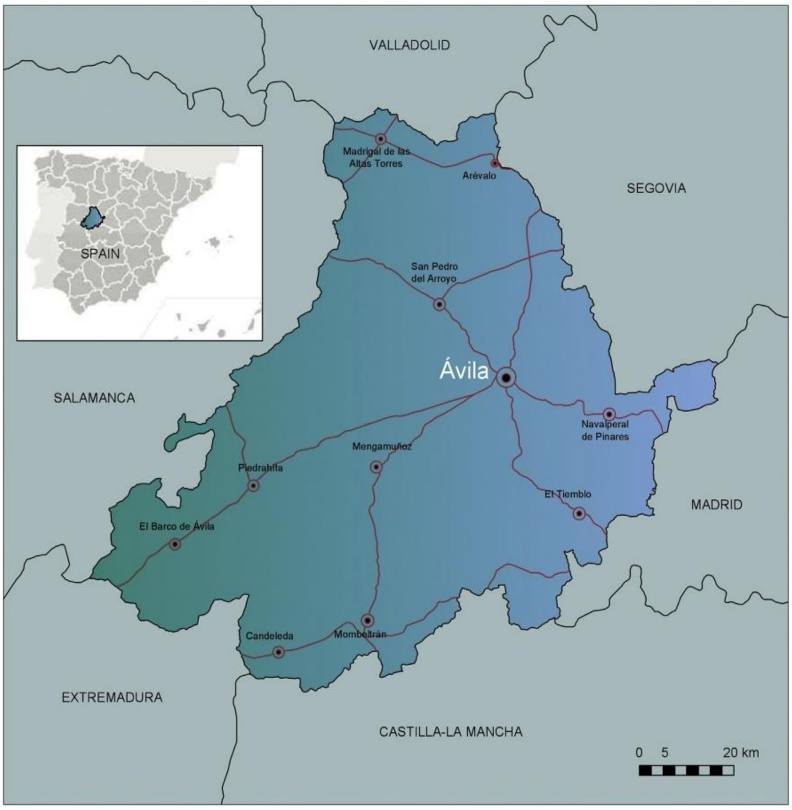


**Fig. 1.** Study location, province of Ávila.

**Table 1**
List of principal geologic materials by rock type and by geologic age of the province of Ávila and its area ($m^2$).

| | Geological Formation | | Area ($m^2$) | Percentage (%) |
|---|---|---|---|---|
| ROCKS | | Granitic Rocks | 4727371144.80 | 58.73 |
| | 1 | Granite | 4141732.90 | 4.65 |
| | 2 | Monzogranite | 351222457.10 | 4.36 |
| | 3 | Leucogranite | 278550245.90 | 3.46 |
| | 4 | Granitoid | 519901676.90 | 6.46 |
| | 5 | Granodiorite | 2083912516.00 | 25.89 |
| | 6 | Adamellite | 1119642516.00 | 13.91 |
| | | Metamorphic Rocks | 89364335.27 | 1.11 |
| | 7 | Leuco gneiss | 2787675.83 | 0.03 |
| | 8 | Orto gneiss | 59273484.05 | 0.74 |
| | 9 | Gneiss | 27303175.39 | 0.34 |
| | | Cambrian-low Pre-Cambrian | 440678930.74 | 5.47 |
| | 10 | Slate | 80855662.67 | 1.00 |
| | 11 | Quartzite | 35654498.27 | 0.44 |
| | 12 | Schist | 324168769.80 | 4.03 |
| | | Pre-Arenigiense | 99894327.99 | 1.24 |
| | 13 | Meta-sediment | 99894327.99 | 1.24 |
| SOILS | | Tertiary | 2095838252.00 | 26.03 |
| | 14 | Sand, arkoses, clay, mud and stone | 2095838252.00 | 26.03 |
| | | Quaternary | 597003009.50 | 7.42 |
| | 15 | Terrace, alluvial, glacis | 597003009.50 | 7.42 |
| | | | 8050150000.30 | 100 |

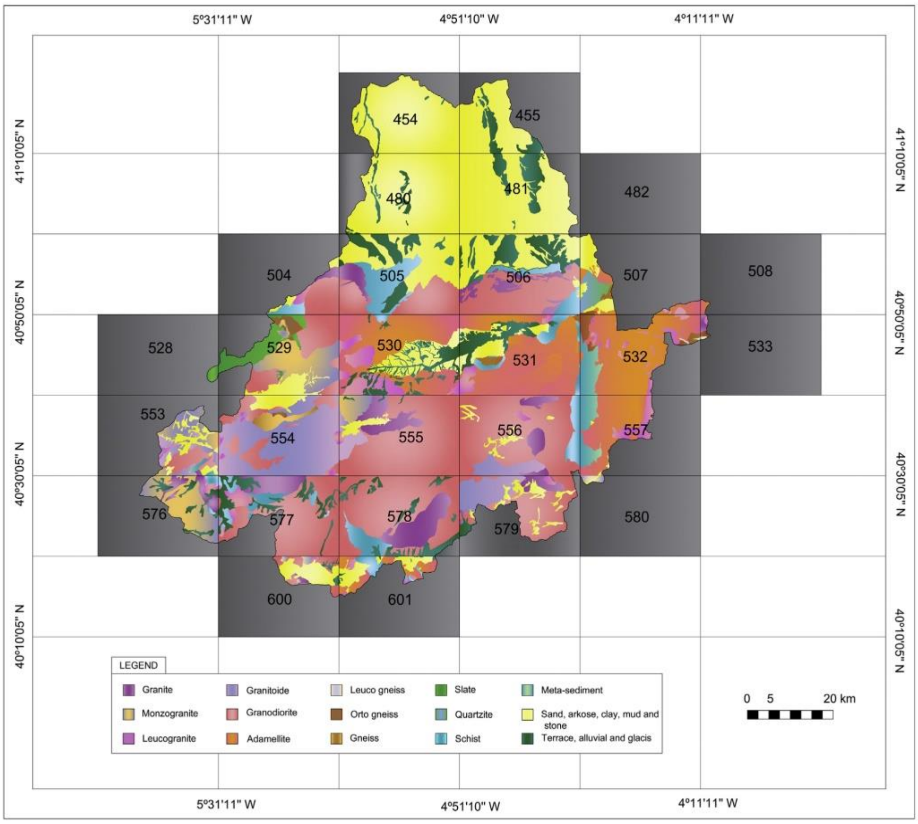


**Fig. 2.** Grids that divide the province of Ávila and its geology.

resistant between the sensor and the sample granular and solid materials. The contact between needle and tested material is guaranteed by putting thermal grease in the hole drilled for the emplacement of the needle.

It is convenient to mention that, RK-1 sensor was previously calibrated before its use by a test tube supplied by the manufacturer.

Despite the fact RK-1 sensor is specifically designed for its use in hard materials like rock or cured concrete, in this work; it was used in rocks but also in soils previously compacted. Before proceeding to use the equipment, the pertinent samples preparation was carried out. The sensor must be able to penetrate into the specimen to be measured (in drilled boreholes in case of solid rocks) or inserted into specially prepared (compacted) samples in case of unconsolidated material. In the case of rocks, samples were prepared in the lab, obtaining cylinder blocks of 5 cm of diameter and length superior to the sensor RK-1 length (6 cm), where a hole has been made with the purpose of containing the sensor. On the contrary, soils were compacted in *Proctor* essay conditions in order to reproduce the compaction state of these materials to greater depths, where, due to pressure and temperature effects, the compaction conditions differ from those in the surface where samples were taken. Once the soil was compacted in the appropriate mold, sensor RK-1 was directly introduced in the sample obtained from the execution of the mentioned *Proctor* essay [UNE 103-500-94, 1994]. As this essay specifies, soil with defined water content was introduced in Proctor mold in three steps and 26 hits were made on each one of the three layers in the mold with the corresponding tenderizer. After carrying out this essay, the soil gets the compaction in Proctor conditions for certain water content.

The degree of consolidation of the sampled materials was the one resulting from the explained Proctor essay.

In respect to anisotropy factors, measurements with KD2 Pro have been carried out only in perpendicular direction to the layers, considering a horizontal position of them, similar to the one we would find in a hole given the tectonics of the region. In this way, anisotropy factors were not considered.

Fig. 4 shows the procedure followed from the data collection in the land to the measuring of the thermal conductivity parameter in the laboratory.

Location of materials (presented in Table 1) on the basis of geological information and collection of representative samples of each of them. Geographical coordinates were written down with the aim of verifying that the location of these samples coincides with the points marked in the map represented in Fig. 3.

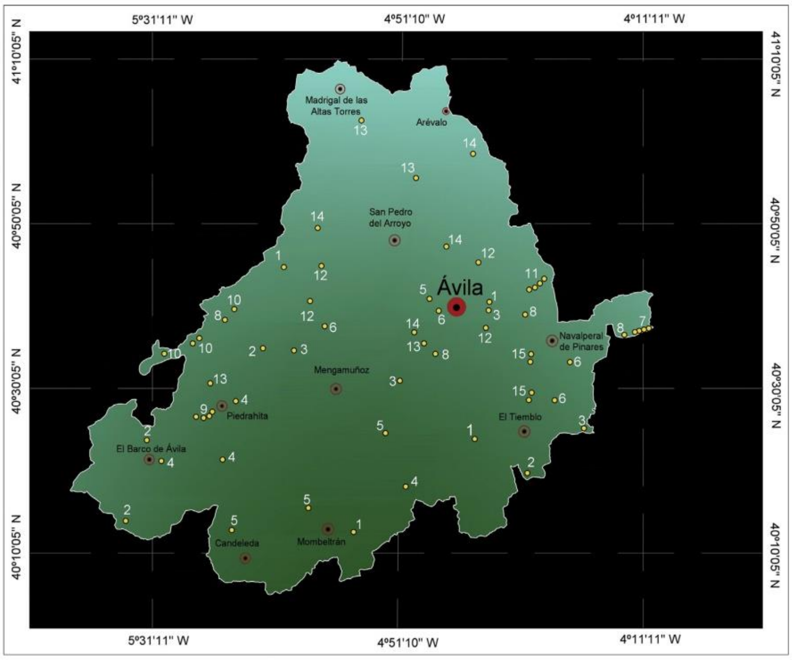


**Fig. 3.** Sampling point's position for the four samples of each material (rock types/formations 1–15, see Table 1).

(a) Rocks drilling and extraction of samples of 5 cm of diameter and variable length, depending on the rock block size.
(b) Carving of samples by using a cutting-machine supplied with diamond disk. The length of these samples was equal or longer than 6 cm so that the needle probe RK-1 (6 cm length) is totally inside them.
(c) Samples obtained and surplus rocky material.

Drilling of a hole in every rocky sample where the sensor RK-1 was introduced for the measuring of thermal conductivities. In all cases this hole was of 6 cm length and 3.9 mm of diameter, dimensions coinciding with the needle probe dimensions.

(d) Positioning of thermal grease in the samples holes to improve the contact and the thermal transfer between sensor and rock.
(e) Installation of the KD2 Pro and sensor RK-1 in the corresponding rock sample and measuring of the thermal conductivity parameter. The read time of this sensor is approximately 10 min.

KD2 Pro and sensor RK-1 measuring the thermal conductivity of a soil in the *Proctor* mold where the compaction of this material was previously made in the conditions stablished by the law of this essay.

Three measuring of the thermal conductivity parameter were made for each rocky sample and in the case of soils, three measuring for each sample and three different humidity states, modifying the water content of the sample. These there humidity states were established by determining in first place the optimal humidity of each soil and then selecting three humidity values next to this optimal humidity belonging to the ascending phase of Proctor essay, where an increase of humidity also increases the density of the soil sample. Once known the optimal humidity of each soil, samples were dried in a laboratory heater to 105 °C during a week to then add a certain quantity of water (different for each humidity state and guaranteeing not to reach the optimal humidity). By differences of weight between dry and wet samples, densities were calculated. The accuracy of these measurements depends on the electronic scale used, which was able to provide five significant digits.

Given that samples were collected in surface from rocky outcrops, measurements with KD2 Pro provided thermal conductivity values from surface, that is to say, the thermal conductivity of the rocks along the entire borehole heat exchanger cannot be determined with the present methodology. Despite this fact, these measurements constitute a good basis in the calculation of a geothermal heat pump in special if there is not the possibility of carrying out a TRT. Moreover, according with the information of different holes provided by the Geological and Mining Institute of Spain "*IGME*", there is a high concordance between rocks in surface and in depth which means that data obtained in this research from surface samples offer extended information about the thermal conductivity of the entire borehole, although never as complete as the one supplied by a TRT.

### 2.3.2. ThermoMap

Given that the equipment KD2 Pro used in the measuring of thermal conductivities in this work is not specifically designed to be used in soils, the calculation of this thermal conductivity property in these materials was concurrently carried out utilizing ThermoMap software. In this way, it was possible to compare the thermal


**Fig. 4.** Sequence of the process of thermal conductivity measurement (a–h, see text).

conductivity values in soils obtained through two different procedures: KD2 Pro and ThermoMap.

ThermoMap is a project focused on the cartography of superficial geothermal resources areas that offers ground and ground water data to a certain depth (0–10 m), offering information about the geothermal potential of Europe. The project harmonizes a group of pre-existing data, related to the ground, climate, and geographical, hydrogeological and geological data with standardized methods. Also, by the data collection in fourteen European areas, ThermoMap has designed a web GIS (Geographical Information System) where users can access to the geothermal potential of these countries. If the area is not considered by this GIS (like the area studied in the present study), ThermoMap additionally has a calculator that allows estimating the thermal conductivity of a certain soil. Therefore, a series of specific parameters of the material in question are required by the application, such as density (g/cm$^3$), humidity (%) and content of sands, clays and muds expressed in percentage (%).

**Table 2**
Values of thermal conductivity of the rock types of Ávila measured with KD2 Pro.

| Geological Formation | Thermal Conductivity (W/mK) | | | | | |
|---|---|---|---|---|---|---|
| 1. Granite | $K_1$ | $K_2$ | $K_3$ | $K_{1-3medium}$ | $\sigma$ | $K_{Medium-Total}$ |
| $M_1$ | 2.577 | 2.647 | 2.594 | 2.606 | 0.036 | 2.650 |
| $M_2$ | 2.665 | 2.666 | 2.651 | 2.661 | 0.008 | |
| $M_3$ | 2.652 | 2.657 | 2.664 | 2.658 | 0.006 | |
| $M_4$ | 2.652 | 2.685 | 2.686 | 2.674 | 0.019 | |
| 2. Monzogranite | $K_1$ | $K_2$ | $K_3$ | $K_{1-3medium}$ | $\sigma$ | $K_{Medium-Total}$ |
| $M_1$ | 2.392 | 2.314 | 2.471 | 2.392 | 0.078 | 2.533 |
| $M_2$ | 2.668 | 2.574 | 2.523 | 2.588 | 0.073 | |
| $M_3$ | 2.525 | 2.788 | 2.583 | 2.632 | 0.138 | |
| $M_4$ | 2.577 | 2.463 | 2.518 | 2.519 | 0.057 | |
| 3. Leucogranite | $K_1$ | $K_2$ | $K_3$ | $K_{1-3medium}$ | $\sigma$ | $K_{Medium-Total}$ |
| $M_1$ | 2.755 | 2.872 | 2.784 | 2.804 | 0.061 | 2.829 |
| $M_2$ | 2.881 | 2.889 | 2.849 | 2.873 | 0.021 | |
| $M_3$ | 2.827 | 2.802 | 2.802 | 2.810 | 0.014 | |
| $M_4$ | 2.787 | 2.846 | 2.849 | 2.827 | 0.034 | |
| 4. Granitoid | $K_1$ | $K_2$ | $K_3$ | $K_{1-3medium}$ | $\sigma$ | $K_{Medium-Total}$ |
| $M_1$ | 2.668 | 2.751 | 3.086 | 2.835 | 0.221 | 2.633 |
| $M_2$ | 2.381 | 2.430 | 2.435 | 2.415 | 0.029 | |
| $M_3$ | 2.643 | 2.649 | 2.641 | 2.644 | 0.004 | |
| $M_4$ | 2.656 | 2.556 | 2.698 | 2.637 | 0.073 | |
| 5. Granodiorite | $K_1$ | $K_2$ | $K_3$ | $K_{1-3medium}$ | $\sigma$ | $K_{Medium-Total}$ |
| $M_1$ | 2.112 | 2.198 | 2.187 | 2.166 | 0.047 | 2.207 |
| $M_2$ | 2.206 | 2.285 | 2.296 | 2.262 | 0.049 | |
| $M_3$ | 2.147 | 2.158 | 2.215 | 2.173 | 0.036 | |
| $M_4$ | 2.242 | 2.178 | 2.256 | 2.225 | 0.041 | |
| 6. Adamellite | $K_1$ | $K_2$ | $K_3$ | $K_{1-3medium}$ | $\sigma$ | $K_{Medium-Total}$ |
| $M_1$ | 2.693 | 2.565 | 2.641 | 2.633 | 0.064 | 2.855 |
| $M_2$ | 2.976 | 2.937 | 2.956 | 2.956 | 0.019 | |
| $M_3$ | 2.945 | 3.147 | 2.825 | 2.972 | 0.162 | |
| $M_4$ | 2.806 | 2.960 | 2.809 | 2.858 | 0.008 | |
| 7. Leuco gneiss | $K_1$ | $K_2$ | $K_3$ | $K_{1-3medium}$ | $\sigma$ | $K_{Medium-Total}$ |
| $M_1$ | 2.560 | 2.505 | 2.534 | 2.533 | 0.027 | 2.452 |
| $M_2$ | 2.364 | 2.358 | 2.425 | 2.382 | 0.037 | |
| $M_3$ | 2.432 | 2.441 | 2.449 | 2.441 | 0.008 | |
| $M_4$ | 2.440 | 2.456 | 2.455 | 2.450 | 0.009 | |
| 8. Orthogneiss | $K_1$ | $K_2$ | $K_3$ | $K_{1-3medium}$ | $\sigma$ | $K_{Medium-Total}$ |
| $M_1$ | 2.152 | 2.599 | 2.359 | 2.370 | 0.050 | 2.590 |
| $M_2$ | 2.632 | 2.596 | 2.655 | 2.628 | 0.030 | |
| $M_3$ | 2.668 | 2.653 | 2.675 | 2.665 | 0.011 | |
| $M_4$ | 2.669 | 2.666 | 2.751 | 2.695 | 0.048 | |
| 9. Gneiss | $K_1$ | $K_2$ | $K_3$ | $K_{1-3medium}$ | $\sigma$ | $K_{Medium-Total}$ |
| $M_1$ | 2.903 | 2.987 | 2.859 | 2.916 | 0.065 | 2.900 |
| $M_2$ | 2.713 | 2.992 | 2.720 | 2.808 | 0.159 | |
| $M_3$ | 3.001 | 3.023 | 3.019 | 3.014 | 0.012 | |
| $M_4$ | 2.853 | 2.875 | 2.852 | 2.860 | 0.013 | |
| 10. Slate | $K_1$ | $K_2$ | $K_3$ | $K_{1-3medium}$ | $\sigma$ | $K_{Medium-Total}$ |
| $M_1$ | 2.851 | 2.952 | 2.911 | 2.905 | 0.051 | 3.102 |
| $M_2$ | 3.178 | 3.118 | 3.210 | 3.169 | 0.002 | |
| $M_3$ | 3.179 | 3.258 | 3.165 | 3.201 | 0.050 | |
| $M_4$ | 3.227 | 3.060 | 3.112 | 3.133 | 0.085 | |
| 11. Quartzite | $K_1$ | $K_2$ | $K_3$ | $K_{1-3medium}$ | $\sigma$ | $K_{Medium-Total}$ |
| $M_1$ | 2.880 | 2.874 | 2.926 | 2.893 | 0.028 | 3.257 |
| $M_2$ | 2.933 | 2.972 | 3.160 | 3.022 | 0.121 | |
| $M_3$ | 3.187 | 3.247 | 3.264 | 3.233 | 0.040 | |
| $M_4$ | 3.304 | 3.248 | 3.678 | 3.410 | 0.055 | |
| 12. Schist | $K_1$ | $K_2$ | $K_3$ | $K_{1-3medium}$ | $\sigma$ | $K_{Medium-Total}$ |
| $M_1$ | 3.024 | 3.026 | 3.036 | 3.029 | 0.006 | 3.019 |
| $M_2$ | 3.009 | 3.011 | 3.009 | 3.010 | 0.001 | |
| $M_3$ | 3.005 | 3.031 | 3.007 | 3.014 | 0.014 | |
| $M_4$ | 3.020 | 3.025 | 3.026 | 3.024 | 0.003 | |
| 13. Meta-sediment | $K_1$ | $K_2$ | $K_3$ | $K_{1-3medium}$ | $\sigma$ | $K_{Medium-Total}$ |
| $M_1$ | 2.368 | 2.281 | 2.343 | 2.331 | 0.045 | 2.425 |
| $M_2$ | 2.442 | 2.478 | 2.537 | 2.486 | 0.048 | |
| $M_3$ | 2.428 | 2.476 | 2.421 | 2.442 | 0.030 | |
| $M_4$ | 2.487 | 2.331 | 2.504 | 2.441 | 0.095 | |

Thermal conductivity depends largely on the pores size and its distribution as well as the saturation level. To calculate the thermal conductivity, ThermoMap considers these two assumptions:

- For percentages of sand >50%, thermal conductivity is computed as:

$$k = 0.1442 \left(0.7 \left(lg \frac{PSD}{BD}\right) + 0.4\right) 10^{(0.6243BD)} \quad (4)$$

- For percentages of sand <50%, thermal conductivity is computed as:

$$k = 0.1442\left(0.9\left(lg\frac{PSD}{BD}\right) - 0.2\right)10^{(0.6243BD)} \quad (5)$$

Where:
$k$ = thermal conductivity (W/mK)
$PSD$ = distribution of pores size (% per volume)
$BD$ = bulk density (g/cm$^3$)

According to the texture class of the material, one or another equation is selected and applied in the corresponding calculation of the soil, using the *PSD* factor deduced from the hydrological state of the system and defining the bulk density values *BD* (usually 1.3 g/cm$^3$ for the depth interval 0–3 m, 1.5 g/cm$^3$ for the depth interval 3–6 m and 1.8 g/cm$^3$ for the depth interval 6–10 m) (Bertermann et al., 2013).

This application incorporates automatically the climatic parameters of the area in question so it is only necessary to introduce the three data of density, humidity and soil grading, indicating this last parameter by a textural triangle.

ThermoMap calculator offers the possibility of selecting the depth where the material, whose thermal conductivity wants to be obtained, is, with values comprised between 0 m and 10 m. In this case, as it has already been mentioned, depth was not defined, because, although soil samples have been taken in surface, soils were compacted to simulate its state to greater depth. In this way, when introducing density values in this application, we are giving information about its depth, because, to higher compaction the density of the material is also greater, so the high compaction of soils increases its density and with that a position, to a depth typical of a very low enthalpy geothermal energy ( < 100 m) submitted to internal temperatures and pressures, is being simulated (Abu-Hamdeh and Reeder, 2000).

In Section 3.2. Estimating thermal conductivities with ThermoMap, thermal conductivities of each soil sample were estimated by this procedure and for each of them three estimations were made, corresponding to three different humidity states and density.

## 3. Results and discussion

### 3.1. Measuring with KD2 Pro

Following, Table 2 shows the results of thermal conductivities measurements of the rocky samples taken to laboratory by the use of KD2 Pro. As it has been mentioned throughout this paper, four samples of each one of the rocks types of the province of Ávila were collected. As Table 2 shows, three measurements of each sample were made ($K_1$, $K_2$, $K_3$), the medium value of these three data was calculated ($K_{1\text{-}3medium}$) and finally the medium value of the group of values of all the samples of each formation ($K_{MediumTotal}$).

Additionally, standard deviation ($\sigma$), which represents the deviation of the measured values ($K_1, K_2, K_3$) with respect to the medium value ($K_{1\text{-}3medium}$), is also presented in Table 2 (Bevington and Robinson, 1992).

Table 3 presents the results of thermal conductivity of soils measured equally with the KD2 Pro. In this case, for each of the four samples of each soil, three different humidity conditions ($H_1$, $H_2$, $H_3$) were reproduced, making three measuring for each sample and humidity state and calculating as in the case of rocks, the medium values of the three values measures per sample and humidity ($K_{1\text{-}3medium}$) and the medium value of the group of samples and for each humidity ($K_{MediumTotal}$).

Analyzing both Tables 2 and 3, a series of observations can be deduced:

- The highest values of thermal conductivity belong to quartzite, slates and schist formations, that is to say, these materials would be the most appropriate ones to conduce the heat and, therefore, they would give the best results of efficiency in a geothermal installation. It would make possible to reduce the heat pump power and the total drilling length.
- The highest standard deviations have been obtained for samples of granitites, adamellites, gneiss and terraces what indicates that, in these rocks types the measuring process with sensor RK-1 experimented higher variations possibly due to anomalies in the contact of this sensor with the rock because of changes at the thermal grease distribution.

**Table 3**
Values of thermal conductivity of the soils of Ávila measured with KD2 Pro.

| | Geological Formation | Thermal Conductivity (W/mK) | | | | | |
|---|---|---|---|---|---|---|---|
| | Sands, clays and muds | $K_1$ | $K_2$ | $K_3$ | $K_{1\text{-}3medium}$ | $\sigma$ | $K_{Medium\text{-}Total}$ |
| $H_1$ = 6.32% | M 1 | 1.444 | 1.405 | 1.456 | 1.435 | 0.027 | 1.502 |
| | M 2 | 1.421 | 1.498 | 1.499 | 1.473 | 0.045 | |
| | M 3 | 1.587 | 1.502 | 1.599 | 1.563 | 0.053 | |
| | M 4 | 1.506 | 1.589 | 1.521 | 1.539 | 0.044 | |
| $H_2$ = 10.97% | M 1 | 1.804 | 1.621 | 1.723 | 1.716 | 0.092 | 1.834 |
| | M 2 | 2.227 | 2.156 | 2.063 | 2.149 | 0.082 | |
| | M 3 | 1.900 | 1.897 | 1.841 | 1.879 | 0.033 | |
| | M 4 | 1.612 | 1.583 | 1.584 | 1.593 | 0.016 | |
| $H_3$ = 15.74% | M 1 | 2.301 | 2.444 | 2.406 | 2.384 | 0.074 | 2.434 |
| | M 2 | 2.438 | 2.517 | 2.423 | 2.459 | 0.050 | |
| | M 3 | 2.389 | 2.352 | 2.439 | 2.393 | 0.044 | |
| | M 4 | 2.530 | 2.509 | 2.464 | 2.501 | 0.034 | |
| | Terraces, alluvial, glacis | $K_1$ | $K_2$ | $K_3$ | $K_{1\text{-}3medium}$ | $\sigma$ | $K_{Medium\text{-}Total}$ |
| $H_1$ = 6.32% | M 1 | 1.939 | 1.884 | 1.920 | 1.914 | 0.028 | 1.882 |
| | M 2 | 1.898 | 1.903 | 1.842 | 1.881 | 0.034 | |
| | M 3 | 1.849 | 1.850 | 1.903 | 1.867 | 0.031 | |
| | M 4 | 1.838 | 1.877 | 1.882 | 1.866 | 0.024 | |
| $H_2$ = 10.97% | M 1 | 1.793 | 1.653 | 1.857 | 1.768 | 0.104 | 2.041 |
| | M 2 | 2.430 | 2.251 | 2.217 | 2.299 | 0.114 | |
| | M 3 | 2.210 | 2.353 | 2.210 | 2.258 | 0.082 | |
| | M 4 | 2.071 | 1.736 | 1.711 | 1.839 | 0.201 | |
| $H_3$ = 15.74% | M 1 | 2.052 | 2.102 | 2.156 | 2.103 | 0.052 | 2.125 |
| | M 2 | 1.996 | 1.998 | 2.115 | 2.036 | 0.068 | |
| | M 3 | 2.205 | 2.187 | 2.203 | 2.198 | 0.010 | |
| | M 4 | 2.158 | 2.146 | 2.187 | 2.164 | 0.021 | |

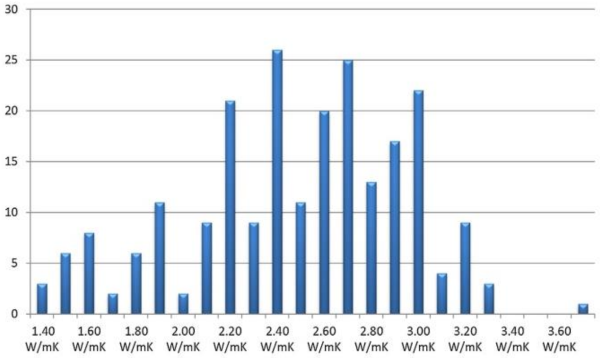


**Fig. 5.** Frequency distribution of measured conductivities.

- The highest differences among the four samples of each rock type were obtained at monzogranites, granitites, adamellites, ortogneiss, quartzite and terraces. This fact means that, these rocks types are more heterogeneous in composition or structural state and therefore, they exhibit thermal conductivity variations.
- In every case studied in Table 3, it can be concluded that, for a higher humidity content of the soil sample, thermal conductivity is also higher. This fact is derived from the pores filled with water; this substance has higher conductivity than the air, so the total soil conductivity also increases.
- Formations 14 and 15 (soils) do not exhibit significant differences in thermal conductivity.

Fig. 5 shows the distribution of the thermal conductivity measurements carried out on the solid rock samples by the use of the equipment KD2 Pro and the corresponding sensor RK-1. Analyzing this distribution, it can be observed that the most frequent value is 2.40 W/mK followed by 2.70 W/mK and 3.00 W/mK. These values represent quite high thermal conductivities that point out the suitable capacity of these materials to conduct the heat.

### 3.2. Estimating thermal conductivities with ThermoMap

By the thermal conductivity calculator of ThermoMap, thermal conductivities of the samples of each soil that occur in the province of Ávila were estimated. In this way, it is viable to make a comparative of the two methods considered for the calculation of this parameter in soils.

As it has already been mentioned, this application requires three parameters of the soils in question: humidity, density and soil grading. Firstly, both bulk density and water content of each sample were defined with the object of simulating the conditions to which soil would be to depths typical of very low enthalpy geothermal resources (<100 m). Thus, three humidity conditions ($H_1$, $H_2$, $H_3$) were reproduced on the samples of each soil studied in the present paper and densities of these samples were calculated [UNE 103-300-93, 1993].

The last factor to be determined is the percentage of sand, mud and clay of these soils. To this end, a gradation test was carried out on each one of them according to the procedure considered in the grading essay by sieve [UNE 103-101/95, 1995]. As a result of these essays, it was possible to know the soils grading to classify them according to Casagrande's Classification (Bjerrum et al., 1973). By way of example, Figs. 6 and 7 show the grading curves obtained from the grading essays by sieve on the sample 1 ($M_1$) of both soils and its classification.

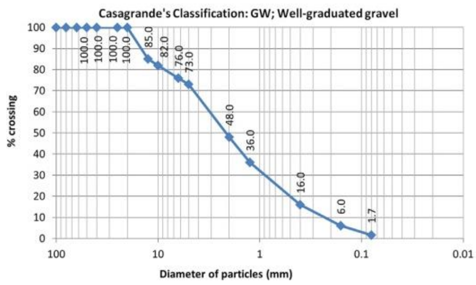


**Fig. 6.** Grading curve of sample 1 from formation 14: Sands, clays and muds.

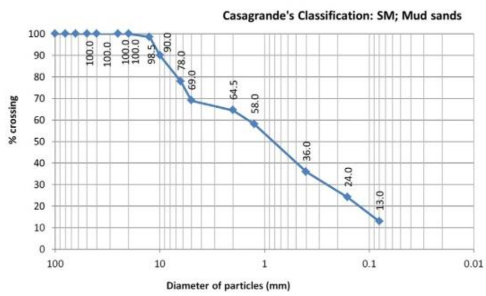


**Fig. 7.** Grading curve of sample 1 from formation 15: terraces, alluvial and glacis.

In this way, after carrying out the grading essay to each sample from formation 14, it was concluded that:

- $M_1$ = Well graduated stones, mixtures of stones and sands with few or none thin particles (GW)
- $M_2$ = Mud stones, mixtures of stones, sand and mud (GM)
- $M_3$ = Mud sands, mixtures of sand and mud (SM)
- $M_4$ = Well graduated stones, mixtures of stones and sands with few thin particles or none (GW)

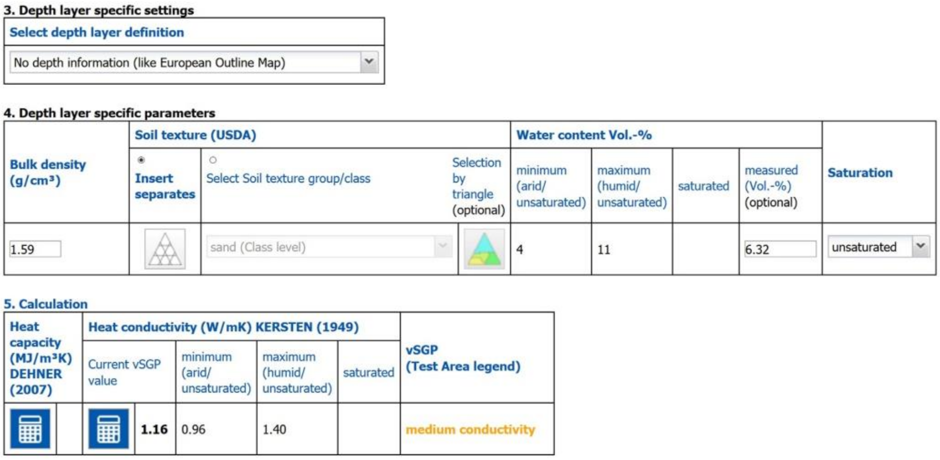


**Fig. 8.** Example of calculation of thermal conductivity of sample 1 from formation 14 by ThermoMap.

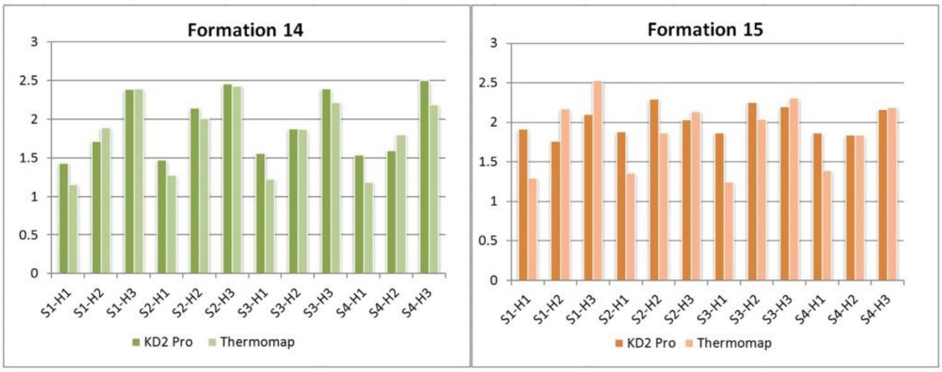


**Fig. 9.** Comparative thermal conductivities obtained by KD2 Pro-vs. ThermoMap.

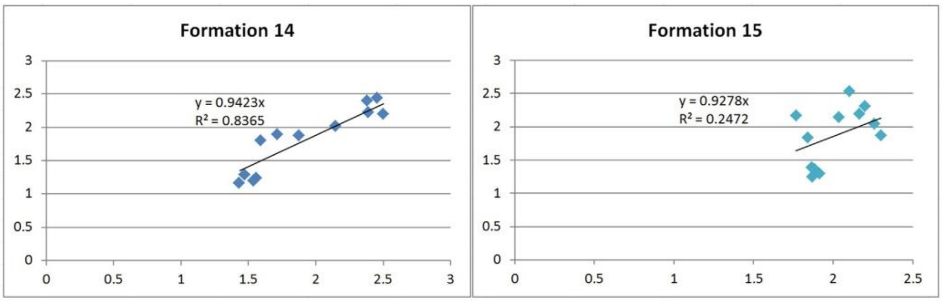


**Fig. 10.** ThermoMap results against KD2 Pro results with the regression coefficient $R^2$.

**Table 4**
Thermal conductivities of samples from formation 14 calculated by ThermoMap.

| | Formation 14: sands, clays and muds | | |
|---|---|---|---|
| | Humidity | Density (gr/cm$^3$) | Thermal Conductivity (W/mK) |
| Sample 1 | $H_1$ | 1.59 | 1.16 |
| | $H_2$ | 1.83 | 1.89 |
| | $H_3$ | 1.90 | 2.31 |
| Sample 2 | $H_1$ | 1.67 | 1.28 |
| | $H_2$ | 1.88 | 2.01 |
| | $H_3$ | 1.94 | 2.43 |
| Sample 3 | $H_1$ | 1.64 | 1.23 |
| | $H_2$ | 1.82 | 1.87 |
| | $H_3$ | 1.87 | 2.22 |
| Sample 4 | $H_1$ | 1.61 | 1.19 |
| | $H_2$ | 1.79 | 1.80 |
| | $H_3$ | 1.86 | 2.19 |

**Table 5**
Thermal conductivities of samples from formation 15 calculated by ThermoMap.

| | Formation 15: terraces, alluvial and glacis | | |
|---|---|---|---|
| | Humidity (%) | Density (gr/cm$^3$) | Thermal Conductivity (W/mK) |
| Sample 1 | $H_1$ | 1.68 | 1.30 |
| | $H_2$ | 1.94 | 2.17 |
| | $H_3$ | 1.97 | 2.53 |
| Sample 2 | $H_1$ | 1.72 | 1.36 |
| | $H_2$ | 1.82 | 1.87 |
| | $H_3$ | 1.84 | 2.14 |
| Sample 3 | $H_1$ | 1.65 | 1.25 |
| | $H_2$ | 1.89 | 2.04 |
| | $H_3$ | 1.90 | 2.31 |
| Sample 4 | $H_1$ | 1.74 | 1.39 |
| | $H_2$ | 1.81 | 1.84 |
| | $H_3$ | 1.86 | 2.19 |

In this case, after completing the grading essay of formation 15 to each one of the samples, it was deduced that:

- $M_1$ = Mud sands, mixtures of sand and mud (SM)
- $M_2$ = Well graduated sands, sands with stones with few or none thin particles (SW)
- $M_3$ = Mud stones, mixtures of stone, sand and mud (GM)
- $M_4$ = Mud sands, mixtures of sand and mud (SM)

Once the grading compositions of each of the four samples of both materials are known, percentages of stones, sands and thin particles that these formations have, were also determined to be used in the calculator of ThermoMap to estimate thermal conductivities.

After obtaining the three parameters for each soil (density, humidity and soil grading), they have been introduced into ThermoMap calculator.

By way of example, Fig. 8 shows the variables inserted in the application (density, humidity and grading composition) and the result of thermal conductivity obtained for sample 1 from formation 14: *sands, clays and muds.*

Tables 4 and 5 outline this result of thermal conductivity presented in Fig. 9 and the values of thermal conductivity calculated for the rest of humidity states and samples of this same formation and those ones corresponding to the samples of the other soil (formation 15: *terraces, alluvial and glacis*). The term *glacis* is referred to colluvial and erosive sedimentary deposits.

### 3.3. Comparison of results, obtained by KD2 Pro and ThermoMap

Thermal conductivities of samples from the geological formations 14 and 15 of the Ávila region (soils) obtained with KD2 Pro were compared with ThermoMap estimations for same locations. As a rule, it can be said that there is a great concordance in the results obtained by both methods. The maximum difference among values resulting from both methods is 0.62 W/mK, being the rest of differences lowers, reaching as minimum difference as 0.001 W/mK. Fig. 9 offers a comparative graphic of the values obtained by each method for the two geological formations and Fig. 10 plots ThermoMap results against KD2 Pro results. In most cases, KD2 Pro presents higher lectures of conductivity than ThermoMap, although the opposite can also be the case. Finally, it can be affirmed that, in spite of the fact that sensor RK-1 of KD2 Pro is not designed to be used in soils, it has supplied acceptable values and similar to the ones obtained with ThermoMap, so it can be considered viable to its use in these conditions.

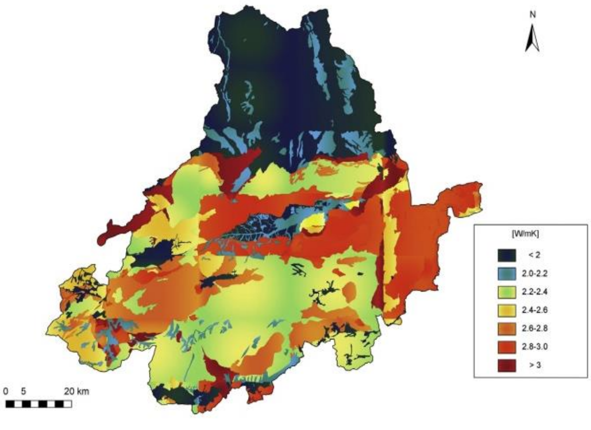


**Fig. 11.** Geothermal map of the Ávila region.

### 3.4. Thermal conductivity map of the province of Ávila

As a result of the analysis and calculation of thermal conductivities of the materials contained in the province of Ávila, a thermal conductivity map of Ávila was produced by grouping of materials according to their thermal conductivity. This map will constitute a valuable tool and help when making decisions about the location and calculation of a very low temperature geothermal installation. A good analysis and study of the area of placing the installation can mean an important economic saving and an improvement of its efficiency. Therefore, the importance of this map, that offers the possibility of locating the most appropriate areas (because of their thermal properties) to utilize this renewable energy, is emphasized. Fig. 11 shows the thermal conductivity map of Ávila. It must be mentioned that several other thermal conductivity maps have been already published in other different regions (Iosifina et al., 2016; Randi et al., 2015).

## 4. Conclusions

The measuring of the thermal conductivity parameter of a series of samples from each geological formation of the province of Ávila has made the production of a thermal conductivity map, possible. The two methods used in this paper were found to be suitable and concordant at the measuring of this thermal property. However, thermal conductivities obtained by ThermoMap are just estimations while measurements with equipment KD2 Pro represent real values of this parameter so this method means the best option to determine the thermal conductivity of rocks and soils.

Within each method, some variations of this parameter were registered in samples belonging to the same geological typology; although insignificant, calculating in each case a medium value to be used in the execution of the geothermal map.

Data collection covering the whole extension and lithology of this region has provided a great variety of thermal information that constitutes an important basis in the pre-design phase of a very low enthalpy geothermal installation. However and given that data were collected in the surface, the thermal conductivity map resulting from the present research has a limitation in its use, that is to say, results are completely reliable to be used in the calculation of the first meters. To greater depths, the most probable is to find the same rocky mass and therefore it would be acceptable the use of the proposed map but it cannot be guaranteed without drilling a hole to take rocky samples from it. For this reason, the use of data presented in this paper is thoroughly recommended and verified for the first meters of drilling but not completely reliable for the rest of the drilling depth. In this way, results should be cross-checked by Thermal Response Tests.

For big projects associated to other types of geothermal energy that require higher drilling lengths, the execution of a Thermal Response Test is highly advisable because it is even more difficult to assure the continuity of the materials from surface.

## Acknowledgments

Authors would like to thank the Department of Cartographic and Land Engineering of the Higher Polytechnic School of Avila, University of Salamanca, for allowing us to use their facilities and their collaboration during the experimental phase of this research. Authors also want to thank the Ministry of Education, Culture and Sport for providing a FPU Grant (Training of University Teachers Grant) to the corresponding author of this paper what has made possible the realization of the present work.

## References

Abu-Hamdeh, N.H., Reeder, R.C., 2000. Soil thermal conductivity: effects of density, moisture, salt concentration, and organic matter. Soil Sci. Soc. Am. J. 64, 1285–1290.

Barry-Macaulay, D., Bouazza, A., Singh, R.M., Wang, B., Ranjith, P.G., 2013. Thermal conductivity of soils and rocks from the Melbourne (Australia) region. Eng. Geol. 164, 131–138.

Bertermann, D., Bialas, C., Morper-Busch, L., Klug, H., Rohn, J., Stollhofen, H., Psyk, M., Jaudin, F., Maragna, C., Einarsson, G., Vikingsson, S., Orosz, L., Jordan, G., Vijdea, A.M., Lewis, M., Lawley, R.S., Latham, A., Declercq, P.Y., Petitclerc, E., Zacherl, A., Arvanitis, A.A., Stefouli, M., 2013. ThermoMap-an open-source web mapping application for illustrating the very shallow geothermal potential in Europe and selected case study areas. EGC2013_SG3-05. In: Proceedings European Geothermal Congress, Pisa, Italy, ISBN 978-2-8052-0226-1.

Bevington, R. Philip, Robinson, Keith, 1992. Data Reduction and Error Analysis for the Physical Sciences, 2nd edition. WCB/McGraw-Hill.

Bjerrum, L., Casagrande, A., Peck, R.B., Skempton, y.A.W., John Wiley and Sons, Terzaghi, K., 1973. Mechanism of Landslides from theory to practice in soil mechanics. V III.

Blázquez, C.S., Martín, A.F., García, P.C., Sánchez Pérez, L.S., del Caso, S.J., 2016. Analysis of the process of design of a geothermal installation. Renewable Energy 89 (1), 188–199.

César, R. Chamorro, José, L. García-Cuesta, María, E. Mondéjar, María, M. Linares, 2014. An estimation of the enhanced geothermal systems potential for the Iberian Peninsula. Renewable Energy 66, 1–14.

Carslaw, H.S., Jaeger, J.C., 1959. Conduction of heat in solid, 2nd edition, Oxford, London.

Clauser, C., Huenges, E., 1995. Thermal conductivity of rocks and minerals. In: Ahrens, T.J. (Ed.), Rock Physics and Phase Relations, a Handbook of Physical Constants. American Geophyscial Union, Washington, pp. 105–126.

Decagon Devices, 2016. KD2 Pro Thermal Properties Analyzer Operator's Manual. Decagon Devices, Inc.

Galgaroa, Antonio, Di Sipiob, Eloisa, Teza, Giordano, Destro, Elisa, De Carli, Michele, Chiesa, Sergio, Zarrella, Angelo, Emmi, Giuseppe, Manzella, Adele, 2015. Empirical modeling of maps of geo-exchange potential for shallow geothermal energy at regional scale. Geothermics 57, 173–184.

Geological and Mining Institute of Spain (IGME), 1972–2003. Geological Mational Mapping (MAGNA).

Iosifina, Iosif Stylianou, Savvas, Tassou, Paul, Christodoulides, Ioannis, Panayides, Georgios, Florides, 2016. Measurement and analysis of thermal properties of rocks for the compilation of geothermal maps of Cyprus. Renewable Energy 88, 418–429.

Jackson, R.D., Taylor, S.A., 1986. Thermal conductivity and diffusivity. Methods of soil analysis, part 1. Phys. Mineral. Methods, 945–956.

Kluitenberg, G.J., Ham, J.M., Bristow, K.L., 1993. Error analysis of the heat pulse method for measuring soil volumetric heat capacity. Soil Sci. Soc. Am. J. 57, 1444–1451.

Peláez, Pedro Casanova, Carnicero, José Manuel Palomar, García, Rafael López, Peragon, Fernando Cruz, 2014. Desarrollo de equipo para la realizacián de test de respuesta tírmica del terreno (TRT) en instalaciones geotírmicas. Dyna 89, 316–324.

Randi, K. Ramstad, Kirsti, Midttømme, Heiko, T. Liebel, Bjørn, S. Frengstad, Bjørn, Willemoes-Wissing, 2015. Thermal conductivity map of the Oslo region based on thermal diffusivity measurements of rock core samples. Bull. Eng. Geol. Environ. 74, 1275–1286.

Shiozawa, S., Campbell, G.S., 1990. Soil thermal conductivity. Remote Sens. Rev. 5, 301–310.

Thermo Map, 2013. ThermoMap MapViewer, web site, Available from http:// geoweb2. sbg.ac.at/thermomap/.

Vijdea, Anca-Marina, Weindl, Christopher, Cosac, Ana, Asimopolos, Natalia-Silvia, Bertermann, David, 2014. Estimating the thermal properties of soils and soft rocks for ground source heat pumps installation in Constanta county, Romania. J. Therm. Anal. Calorim. 118, 1135–1144.